Determination of Kinetic Parameters and Thermal Characteristics of Epoxy Casuarina Bio Composites

R. Nalini Suja[1], B. Sridevi[2,*] and Senthil Muthu Kumar Thiagamani[3,4,5,*]

[1]*Department of Chemistry, Panimalar Engineering College, Chennai 600123,Tamil Nadu, India*

[2]*Department of Chemistry, Presidency College, Chennai-600005, Tamil Nadu, India*

[3]*Department of Mechanical Engineering, Kalasalingam Academy of Research and Education, Krishnankoil–626126, Tamil Nadu, India*

[4]*Department of Mechanical Engineering, INTI International University, Persiaran Perdana BBN, Putra Nilai, 71800 Nilai, Negeri Sembilan, Malaysia*

[5]*Centre for Advanced Composite Materials (CACM) Universiti Teknologi Malaysia, 81310 Skudai, Johor Bahru, Johor, Malaysia*

Abstract: By reinforcing casuarina equisetifolia leaf, a flexible bio fibre, in different volume proportions of 4%, 8%, 12%, 16%, and 20% into the epoxy resin, a bio-based composite was produced utilizing the hand layup method. FT IR spectrum was used to verify the production of epoxy casuarina composite. The produced composites have undergone an extensive thermal investigation using Differential Thermal Analysis (DTA), Thermogravimetric Analysis (TGA), Derivative Thermogravimetric (DTG) study and Differential Scanning Calorimetry (DSC) analysis. It has been observed that increasing the percentage of casuarina fibre content enhances the thermal stability of epoxy resin. Horowitz-Metzger (HM), Broido and Coats-Redfern (CR) models were worked and the result revealed that the decomposition of casuarina epoxy composite followed one Dimensional Diffusion Model with coefficient of correlation value close to 1. The thermodynamic parameters including Activation energy (Ea), frequency factor (A), Gibbs free energy (ΔG), entropy (ΔS) and enthalpy (ΔH) of epoxy casuarina composites were found to increase with increase in fibre contents. This makes the composite more suitable for making high performance engineering material for various applications.

Keywords: Epoxy composites, casuarina leaf fibre, Coats-Redfern(CR), Broido and Horowitz-Metzger(HM) models.

1. INTRODUCTION

The demand for bio composite over synthetic fibre is earning great intrigue among the researchers to produce new composites because of low cost, copious, lightness, biodegradability, environmental sustainability, harmless nature, compatibility nature etc. [1]. Plant sources including banana, kenaf, cotton, sisal, jute, coir, coconut shell powder, groundnut powder, bamboo were predominantly considered as effective fillers by many researchers in order to improve various properties of the resin. In order to extend the use of bio composites for outdoor applications thermal characteristics were exhaustively studied. When studying the walnut, mussel, and hazelnut shells as fillers into composite to pure epoxy resin, it was detected by Kianoosh Zamani *et al*. [2] that the addition of mussel shell intensified the composite's thermal properties. The temperature responses of various natural fibres such as bamboo, agro waste were deciphered by Fei Yao *et al*. [3] and calculated the activation energy in the coverage of 160-170KJ/mol.

Research work published by Tanusree Bera *et al*. [4] highlighted that the glass transition temperature and the initial degradation temperature of plain epoxy was elevated by adding carbon black contents. The convincingness of adding oil palm ash as filler to resin was portrayed by M.S. Ibrahim *et al*. [5]. The heat resistant of composites was escalated with the percentage weight of oil palm filler, possibly as a result of higher filler part penetration into the matrix. Ben Samuel *et al*. [6] figured the Tg of epoxy blended with neem oil was higher than epoxy due to the hindrance of secondary molecules rotation. Experiments coordinated by Parivendhan Inbakumar *et al*. [7] showcased the boost in heat withstanding ability of epoxy composite on adding egg shell. The thermal stability of graphite + PET composites conducted by Basheer *et al*. [8] showed a heave in thermal stability with the addition of graphite. Residual recorded weight was high in nitrogen environment than in air. This surged in residue content with increase in graphite content might due to more carbonaceous content. A higher kinetic energy requirement from the environment, imply surge in the thermal steadiness of polyaniline fly ash composite with dilation in fly ash content [9]. In Subhi A Al-Bayaty *et al*.'s [10] study on the degradation kinetics of epoxy mixed with varying weight percentages (10%, 15%, and 20%) of polystyrene, the reaction was determined to be first order. Higher level of polystyrene content higher the thermal stability, evidenced by the activation energy rising from 74.49 to 96.80 KJ/mol. Researchers Ashraf

*Address correspondence to these authors at the Department of Chemistry, Presidency College, Chennai-600005, Tamil Nadu, India;
E-mail: drbsridevi73@gmail.com
Department of Mechanical Engineering, Kalasalingam Academy of Research and Education, Krishnankoil–626126, Tamil Nadu, India;
E-mail: tsmkumar@klu.ac.in

H. Farha *et al*. [11] believed that improved filler dispersion at high concentrations was the reason for the improvement in thermal performance, Tg, and Ea, upon adding ZnO filler to polystyrene resin. The spherical diffusion (R3) mechanism was rendered to be an appropriate one in the thermal investigation of polycaprolactone melded with maleic anhydride. It had a high R^2 value and soared Ea as the heating rate increased. Thermal property of the mixture made by merging 20% polybutylene and 80% cellulose boosts the activation energy and the reaction rate was noted as second order [12]. The thermal characteristics of modified Kevlar/glass fiber composites rendered an increase in Tg without compromising thermal stability with endothermic peaks at 472^{o}C, 511.9^{o}C and 536^{o}C respectively [13].

Kinetic analysis promotes a better way to understand the thermal characteristic and stability of polymers on adding fillers [14,15]. Expanding the use of polymers in a variety of industry sectors necessitate improving their heat stability. The degradation kinetics of the epoxy resin composites followed a second-order process, determined through the Coats-Redfern formula using a best-fit analysis [16]. Mathematical equations were used in kinetic study relating the frequency factor (A) and activation energy (Ea) furnishes detail about best reaction model for the reaction. The Coats–Redfern model, a prevalent integral method, was recommended in the examination of the coal and biomass. It was found by Ghodsieh *et al*. [17] that the bio hardener accelerated the ΔH as well as the Ea of reaction when the sample composition increased from 10 to 30%. The decomposition mechanisms of the polymer have been analyzed using different reaction models to determine the kinetic data of thermal decomposition. In order to forecast the activity of material under varying operating conditions and to figure out the energy required to begin a chemical reaction, kinetic modelling of reaction was studied by Borsoi *et al*. [18]. Suresh Kumar *et al*. [19] used Broido equation to compute the Ea value of plywood. Compared to simple plywood and water-proof plywood, the fire-retardant plywood has higher Ea in the second degradation stage, indicating that it is substantially more thermally stable and would not catch fire even at high temperature.

Casuarina, a leaf from the family of casuarinaceae was used as bio fibre for this study. As per Vishnu and Revathi's [20] calculations, casuarina has high fibre density, fibre length and fibre wall thickness with the composition of 73% holocellulose and 24% lignin. The connection between the fibre and resin plays a prime role in determining the thermal property. The principal purpose of this study was to explore the feasibility of introducing casuarina bio fibre into epoxy resin to focus the thermal characteristics on varying percentage compositions from 4% to 20%. Model-fitting and model-free methods are used to evaluate kinetic properties, with the model-free method being more reliable for determining Ea and A values, as it uses a model-independent mathematical equation. This paper studies CR, HM and Broido kinetic models and evaluates the best fitted kinetic model during the thermal degradation of epoxy casuarina composites and various thermodynamic parameters such as ΔG, ΔH, ΔS.

2. EXPERIMENTAL PART

2.1. Preparation of Epoxy Casuarina Composite

Epoxy resin (LY556) was used as a matrix material in conjunction with polyamine-type hardener (HY951) in the ratio 10:1.Casuarina leaf fibre with density of 1.05 g/cm^{3}was ground using a ball mill into a grain size ranging approximately from 10 to 25 microns. The fibre and matrix were continuously mixed to ensure uniform dispersion of the fibre. The specimens were formed using a wooden mould measuring 300x300x3 mm. Samples were made by hand layup techniques combined with mild compression methods. Variation in the volume percentage of casuarina leaf fibre in the epoxy matrix was achieved by adjusting it to 4%, 8%, 12%, 16% and 20% v/v in the composite specimens. The interior of the mould was coated with a release agent to facilitate the removal of the cured sample.

2.2. Thermal Studies

Thermogravimetric data was employed using NETZSCH STA 2500 Thermo gravimetric Analyzer to reckon the thermal degradation mode of epoxy casuarina leaf composites. TGA was taken by heating all the prepared epoxy casuarina composites (4% to 20%) from 30^{o}C to 600^{o}C running a heating rate of 10^{o}C / min under continuous nitrogen flow. From the TGA curves of weight loss, different degradation stages were studied. NETZSCH DSC 214 type Differential Scanning Calorimeter was used to examine the onset, mid-point and end point Tg from the peaks drawn in DSC curves.

2.3. Kinetic Models

Kinetic modeling of decomposition combined with the knowledge of activation is essential for predicting the behavior of material under diverse operating conditions and also to determine the energy needed to begin the reaction. The rate of reaction for the thermal degradation of composite under non isothermal state is provided as:

$$g(\propto) = \frac{A}{\beta}\int_0^T e^{\frac{-Ea}{RT}}dT \quad (1)$$

On solving equation (1), when 2RT/E≤ 1, Equation (2) is obtained

$$ln\frac{g(\propto)}{T^2} = ln\frac{AR}{\beta Ea} - \frac{Ea}{RT} \quad (2)$$

g(α) is integral representation of the reaction model as a function of conversion

The details regarding the Coats, Broido and Horowitz methods used in this research are enclosed in Table **1**

T_m implies the temperature at which maximum weight loss rate acquired.

θ=T-Ts, Ts corresponds to maximum loss occurring temperature.

From the slope (-Ea/R) and the intercept ($ln\frac{AR}{\beta Ea}$) of straight line produced by presenting 1000/T on X axis and ln g(α)/T^2 on Y axis in Coats- Redfern equation activation energy (Ea) and frequency factor(A) shall be computed. A linear line with slope = -Ea/R and intercept =$\ln\frac{RATm^2}{Ea\beta}$ is rendered for Broido's plot on plotting ln(ln(1/y)) vs 1/T. The activation energy can be determined from the slope of the linear line, while the frequency factor can be calculated from the intercept. A straight line with slope = -Ea/RTs^{2}will be obtained on plotting $\ln(-\ln(1-\propto))$ vs θ for Horowitz Metzger model.

The following 13 models are used to compare the activation energy of all the percentage compositions of epoxy casuarina leaf composites synthesized.

Origin Pro software was used to perform regression analysis for each of the models listed in Table **2** on all

Table 1: Coats, Broido and Horowitz Equations

Model	Equation	X& Y coordinates	References
Coats- Redfern	$ln\frac{g(\propto)}{T^2} = ln\frac{AR}{\beta Ea} - \frac{Ea}{RT}$	$\propto = \frac{w_o - w_t}{w_o - w_\infty}$	[21]
		X axis = 1/T	
		Y axis = $ln\frac{g(\propto)}{T^2}$	
Broido	$\ln[\ln\left(\frac{1}{y}\right)] = -\left(\frac{Ea}{RT}\right) + \ln\frac{RATm^2}{Ea\beta}$	$y = \frac{w_t - w_f}{w_o - w_f}$	[22]
		X axis= 1/T	
		Y axis= $\ln[\ln\left(\frac{1}{y}\right)]$	
Horowitz-Metzger	$\ln(-\ln(1-\propto)) = \frac{Ea\theta}{RTs^2}$	θ=T-Ts	[23]
		X axis= θ	
		Y axis= $\ln(-\ln(1-\propto))$	

w_o and w_∞ symbolize the initial mass and final mass of the reaction respectively, w_t symbolizes mass at time 't'.

Table 2: Algebraic Expressions for Solid State Mechanism [24]

Models	Code	g(α)
One Dimensional Diffusion(ODD)	D1	α^2
Diffusion control Model (Jander)	D3	$[1-(1-\alpha)^{1/3}]^2$
Diffusion control Model (Crank)	D4	$1-(2/3)\alpha-(1-\alpha)^{2/3}$
1st order Model	F1	-ln (1-α)
2nd order Model	F2	$(1-\alpha)^{-1}-1$
Contracting cylinder Model	R2	$1-(1-\alpha)^{1/2}$
Contracting sphere Model	R3	$1-(1-\alpha)^{1/3}$
Mampel Power Law (n=1/3)	$MPL^{1/3}$	$3[1-(1-\alpha)^{1/3}]$
Mampel Power Law (n=1/2)	$MPL^{1/2}$	$2[1-(1-\alpha)^{1/2}]$
Mampel Power Law (n=2/3)	$MPL^{2/3}$	$3/2[1-(1-\alpha)^{2/3}]$
Avrami-Erofeev Equation (n=2)	A2	$[-\ln(1-\alpha)]^{1/2}$
Avrami-Erofeev Equation (n=3)	A3	$[-\ln(1-\alpha)]^{1/3}$
Avrami-Erofeev Equation (n=4)	A4	$[-\ln(1-\alpha)]^{1/4}$

the produced composites. A reaction model that shows the value of the correlation coefficient (R^2) close to 1 is better than other models. The main decomposition (i.e. high mass loss stage) stage has to be considered for studying the thermal characteristics of composites. The entropy, enthalpy and Gibbs free energy for all the epoxy casuarina composites have been found using the following relations (3)–(5).

$$\Delta S = R \ln (Ah/K_B T) \quad (3)$$

$$\Delta H = Ea - RT \quad (4)$$

$$\Delta G = \Delta H - T\Delta S \quad (5)$$

Where, K_B(Boltzmann constant) = 1.3806×10^{-16} erg/deg/mol

R = 8.314 J/K/mol

h (Planck's constant) = 6.625×10^{-27} erg/sec

3. RESULTS AND DISCUSSION

3.1. IR Spectra

The IR spectrum of neat epoxy, casuarina leaf fibre and the epoxy casuarina composite are shown in Figure **1**. Depending upon the chemical interactions between the functional groups and the physical mixing that takes place during the formation of composite, the composite may exhibit changes in the peaks. In epoxy casuarina composite peak ascertained at 1230cm^{-1} and 1020 cm^{-1} are analogous to the asymmetric aromatic C-O stretching and symmetric aromatic C-O stretching respectively, while the peak at 824cm^{-1} indicates out of plane aromatic -CH deformation. Moreover, the appearance of peak at 1610cm^{-1} specifies the asymmetric stretching vibration of carboxylate ion and C=O stretching is observed at 1680cm^{-1}. Due to the stretching vibration of -OH group, a broader peak is observed at 3350cm^{-1}. This broadening of peak when compared to casuarina can occur due to the formation of hydrogen bonds or other types of intermolecular interactions between the biofiller and the resin.

3.2. Thermogravimetric Analysis

Thermal stability is related to the potential of a material to thwart the degradation process at high temperature. TGA is an extensively accessible technique for assessing thermal stability over a wide temperature range, offering information on how the composite behaves as the temperature gradually increases over time. Figure **2** shows typical thermo gram and their derivative DTG for various percentage compositions of epoxy casuarina leaf fibre composites. The weight loss percentage was scrutinized in relation to temperature ranges of 30 to 600 degrees Celsius using the TGA curves. The decomposition phases, ranges of decomposition, maximum decomposition peak temperature were garnered from the graph. Table **3** provides the summary of degradation temperature for all the stages. Depending on the kinds of fibres, the breakdown of plant fibres proceeds in two to four steps of mass losses at 30°C to 800°C due to the volatilization of cellulose, hemicellulose, pectin, lignin at high temperature [25,26].

All the epoxy casuarina composites underwent three stages of degradation and the mass losses at these stages were noted. The first stage of degradation, a drying stage occurred in 30-290°C temperature range with the mass loss of 6-10 %. The weight of the composite is decreased due to the removal of poorly bound water content and volatile substances. Second stage decomposition started at the temperature around 291^{o}C and completed around 490^{o}C with a major loss in weight of 65-74%. Degradation in this stage is maximum which is due to the presence of hemicelluloses, cellulose. The TG curves confirmed the third stage of dissolution at 491-600^{o}C temperature ranges with the destruction of lignin. The presence of closely associated cross linked polysaccharides in lignin makes it rigid and difficult to decompose during thermal degradation. The mass loss of 5.5 -7.5 % occurred in this third stage degradation. The residual mass formed for all the prepared epoxy casuarina composites ranges from 13.3 to 19.6 % which was far high when compared to 2.77 % the residual mass of epoxy. Higher residue content is also an indication for better thermal stability.

It was noted that the thermal property of epoxy casuarina composite surpassed that of pure epoxy resin. From the curves drawn, it was also clear that the thermal characteristics of composite escalated as the addition of casuarina fibre content from 4% to 20% into the matrix. Similar pattern was also observed in poly ester composite with the increase in oil palm ash filler content by M.S. Ibrahim *et al*. [5].

Table **4** makes it evident that as the percentage of fibre content increased from 4% to 8%, the composites' decomposition temperatures, which ranged from T_{10} to T_{60}, shifted toward a higher temperature. The maximum decomposition temperature was detected at 356^{o}C, 356.9^{o}C, 357.5^{o}C, 358^{o}C and 359^{o}C for epoxy casuarina composites with 4,8,12,16 and 20 % fibre percentage respectively, which is far high from epoxy without fibre. Tg depends on the interactions between the fibre and the matrix phase. From DSC curves it was detected that the Tg of epoxy + casuarina fibre composites are higher than pure epoxy. The Tg was further improved from 67 to75.5^{o}C when the casuarina

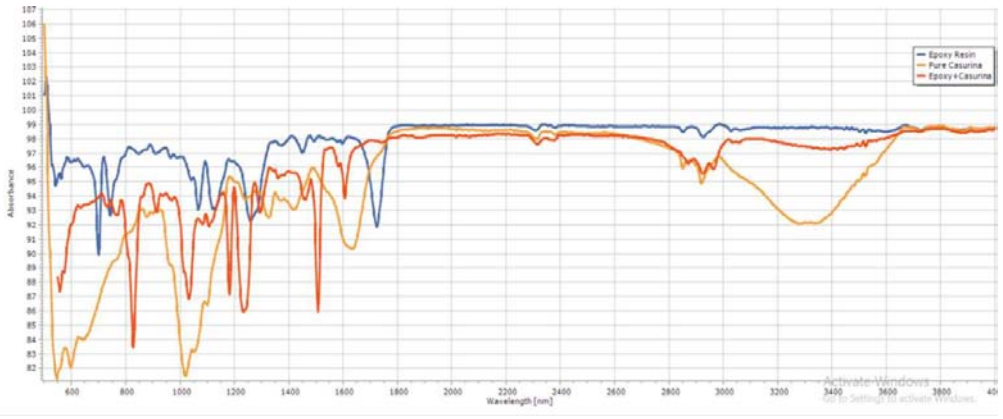

Figure 1: IR spectrum of epoxy, casuarina fibre, casuarina epoxy composites.

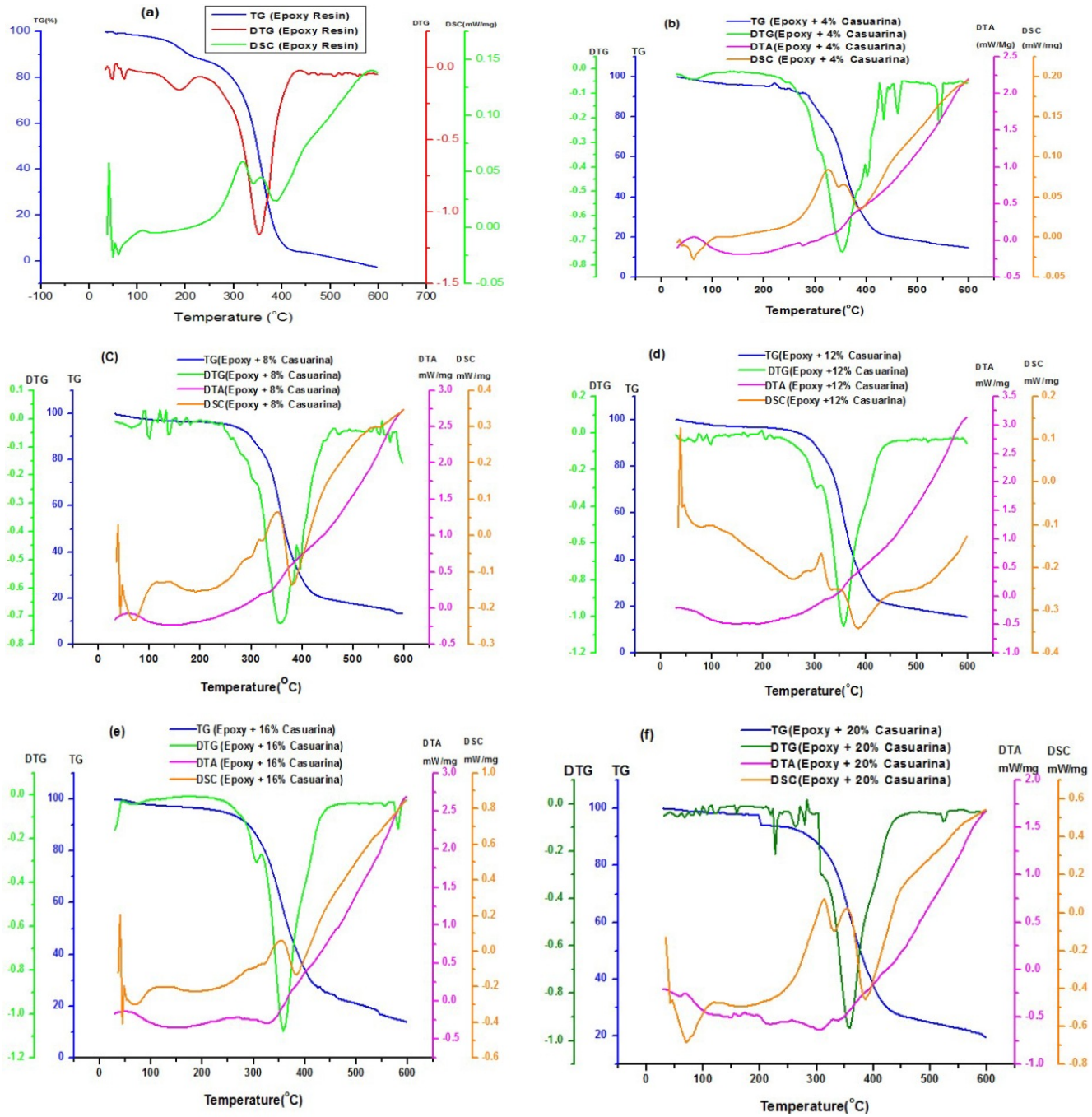

Figure 2: Graph of TG, DTG, DTA and DSC of (**a**). Neat Epoxy (**b**). Epoxy +4% Casuarina composite (**c**). Epoxy +8% Casuarina composite (**d**). Epoxy +12% Casuarina composite (**e**). Epoxy +16% Casuarina composite (**f**). Epoxy +20% Casuarina composite.

Table 3: Various Decomposition Stages of Epoxy Resin and Composites

Samples	Stages	Decomposition Temperature Range (°C)	Mass Loss (%)	Residual Mass (%)
Pure Epoxy	Stage 1	30-254	16.25	2.77
	Stage 2	255-460	75.05	
	Stage 3	461-600	5.93	
Epoxy+4% Casuarina fibre	Stage 1	30-280	8.18	13.63
	Stage 2	281-462	72.16	
	Stage 3	463-600	6.03	
Epoxy+8% Casuarina fibre	Stage 1	30-280	6.9	13.31
	Stage 2	281-464	74.04	
	Stage 3	465-600	5.75	
Epoxy+12% Casuarina fibre	Stage 1	30-282	6.94	14.56
	Stage 2	283-465	72.95	
	Stage 3	466-600	5.55	
Epoxy+16% Casuarina fibre	Stage 1	30-285	9.12	15.22
	Stage 2	286-466	68.03	
	Stage 3	467-600	7.63	
Epoxy+ 20% Casuarina fibre	Stage 1	30-290	10.22	19.68
	Stage 2	291-490	64.53	
	Stage 3	491-600	5.57	

Table 4: Thermal Stability Data of Epoxy Casuarina Leaf Composites

Composites	T_{10}	T_{20}	T_{30}	T_{40}	T_{50}	T_{60}	T max	Tg On set	Tg Mid-point	Tg End point
	(°C)									
Neat Epoxy	207	295	323	338	350	356	355.4	44	59	74
Epoxy+4% Casuarina fibre	288	314	338	352	362	368	356	44	67	90
Epoxy+8% Casuarina fibre	297	328	342	353	365	370	356.9	48	70	92
Epoxy+12% Casuarina fibre	298	332	344	356	368	372	357.5	48	73	98
Epoxy+16% Casuarina fibre	298	327	342	354	369	377	358	50	75	100
Epoxy+20% Casuarina fibre	288	333	348	363	377	385	359	51	75.5	100

fibre content increased from 4% to 20%. The casuarina fibre bonded with the epoxy resin increases the volume and hinders the rotation of molecules. As the fibre content is more, space occupied will be more which will weaken the mobility and further increase the Tg. It is well correlated with the results shown by Ben Samuel et al. [6] on incorporating areca fibre into epoxy matrix.

3.4. Activation Energy Calculation from kinetic modeling

A quantitative analytical technique for figuring out a composite's thermal stability is the kinetic energy activation. The composite's thermal stability is demonstrated by higher Ea. Material exhibiting high Ea can withstand high temperature without degradation and are thermally more stable. The minimal energy required to cause deterioration is assessed by Ea. The second stage of composite's degradation 281-490 °C was selected for kinetics analysis since it reflects the greatest amount of the mass loss when compared to other two stages. CR, HM and Broido methods were used to plot for all the epoxy casuarina composites starting from 4% to 20% volume percentage composition. As discussed in the experimental part group of linear plot of ln $g(\alpha)/T^2$ vs 1000/T is shown in Figure **3** for all the 13 models. As shown in the figure all data fall into straight line with good R^2 value above 0.95. From the linear plots Ea and A were calculated using the formulae mentioned in experimental part. It was discovered that Ea and the frequency factor have a linear connection. Korkut Acikalin [27] recognized this comparable pattern in the study he did on walnut shell. It was also identified by Xian Zhang *et al*. [28] that the introduction of wood floor content from 5 to 20% into HDPE composite increased Ea due to the prevention of

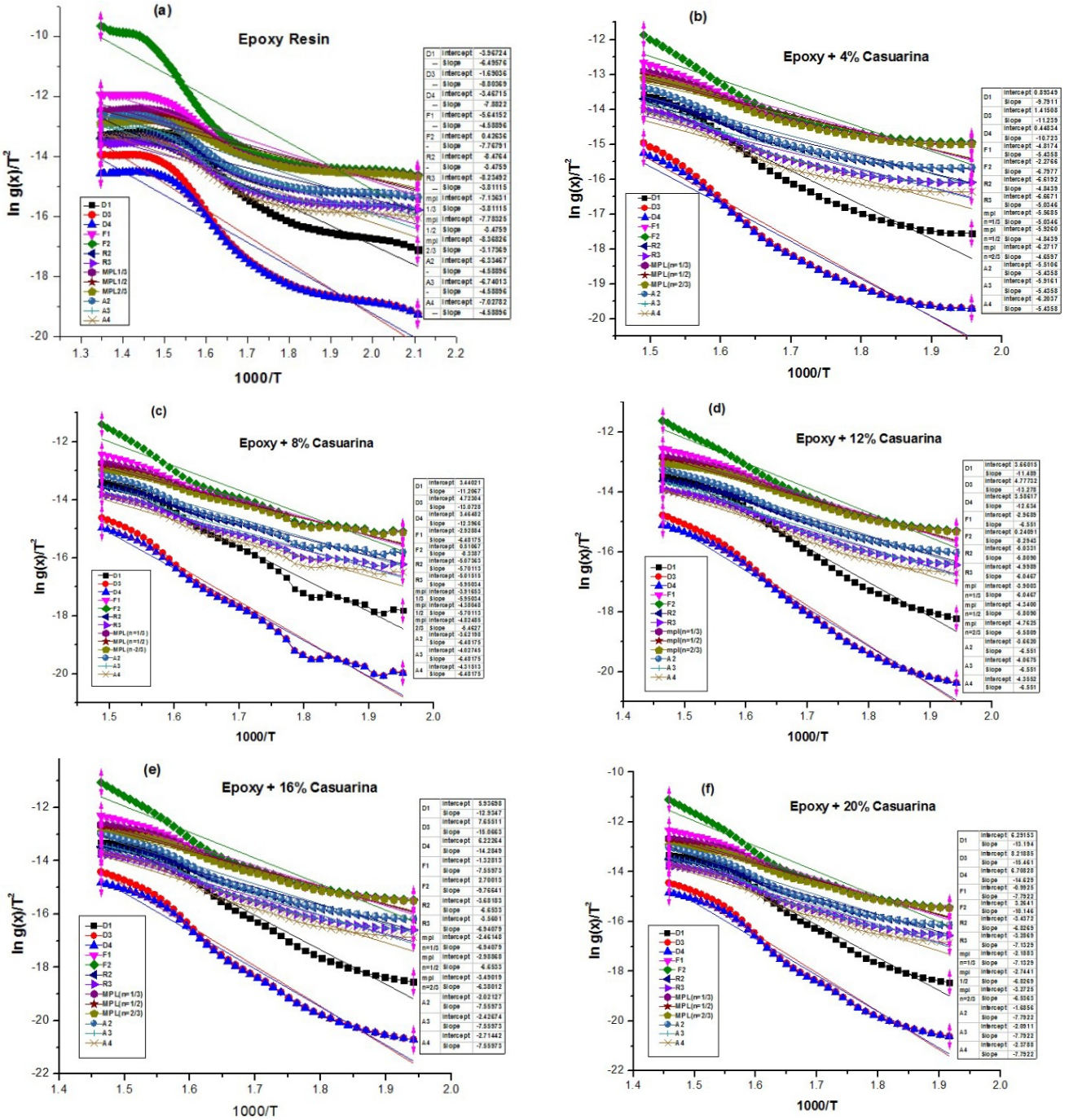

Figure 3: Plot of ln g(x)/T^2vs 1000/T for 13 models (**a**). Neat Epoxy (**b**). Epoxy +4% Casuarina composite (**c**). Epoxy+8% Casuarina composite (**d**). Epoxy+12% Casuarina composite (**e**). Epoxy+16% Casuarina composite (**f**). Epoxy+20% Casuarina composite.

exhibits Broido method graph of ln(ln(1/y)) vs 1000/T for the epoxy casuarina composites. All the data made a linear line with R^2 value close to 1 with the activation energy of 63-73 KJ/mol. Horowitz graph plotted using $\ln(-\ln(1-\propto))$ vs θ for the composites as shown in Figure **4b** is a linear plot with R^2 value close to 1. The activation energy obtained was 69-85KJ/mol.

The addition of casuarina leaf fibre into the epoxy matrix strengthens the polymer chain thereby increasing the activation energy of the epoxy casuarina composites with the increase in fibre content. Presence of high cellulose content in casuarina fibre may also a reason for the large amount of energy requirement to activate molecules in the polymer chain [29]. From the linear plots, the model with highest R^2 value is assigned as the best fitting model. As One-Dimensional Diffusion Model has R^2 value close to 1, it was taken for further calculating various parameters. It was noted that the degradation of epoxy casuarina composite required 81-109KJ/mol energy using ODD(D1) model which depends on the amount of casuarina fibre content present in the composite. This value is identified to increase with increase in casuarina leaf content into the epoxy matrix. Higher the energy of activation higher is the stability of composite.

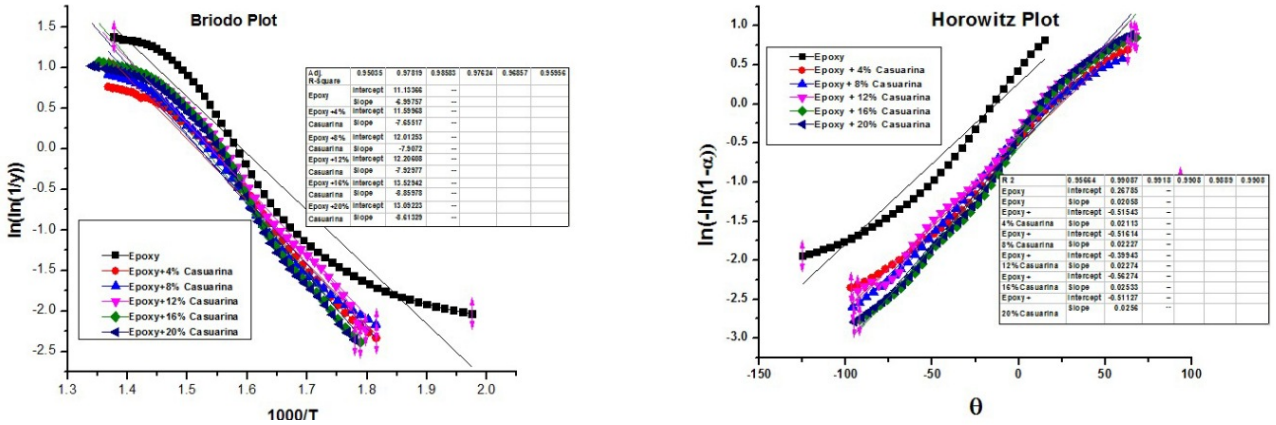

Figure 4: (**a**). Broido plot for Epoxy casuarina composites (**b**). Horowitz plot for Epoxy casuarina composites.

Table 5: Activation Energy and Frequency Factor for Epoxy Casuarina Composites from Various Models

Code	Epoxy Resin	Epoxy + 4% Casuarina	Epoxy + 8% Casuarina	Epoxy+12% Casuarina	Epoxy+16% Casuarina	Epoxy+20% Casuarina
D1	Ea=54	Ea= 81.40	Ea=93.17	Ea= 95.52	Ea= 107.54	Ea= 109.7
	$A=1.23x10^{3}$	$A=2.39x10^{5}$	$A=3.5x10^{6}$	$A=4.47x10^{6}$	$A=4.89x10^{7}$	$A=7.12x10^{7}$
	$R^2=0.9310$	$R^2=0.9573$	$R^2=0.9784$	$R^2=0.9856$	$R^2=0.9804$	$R^2=0.9821$
D3	Ea=73.19	Ea= 93.44	Ea= 108.69	Ea=110.39	Ea=125.26	Ea=128.55
	$A=1.62x10^{4}$	$A=4.63x10^{5}$	$A=1.47x10^{7}$	$A=1.58x10^{7}$	$A=3.18x10^{8}$	$A=5.74x10^{8}$
	$R^2=0.9250$	$R^2=0.9437$	$R^2=0.9714$	$R^2=0.9845$	$R^2=0.9739$	$R^2=0.9783$
D4	Ea=65.53	Ea= 89.15	Ea= 103.37	Ea=105.04	Ea=118.76	Ea=121.63
	$A=2.46x10^{3}$	$A=1.68x10^{5}$	$A=3.96x10^{5}$	$A=4.56x10^{5}$	$A=7.19x10^{7}$	$A=1.19x10^{8}$
	$R^2=0.92887$	$R^2=0.9488$	$R^2=0.9743$	$R^2=0.9856$	$R^2=0.9771$	$R^2=0.9806$
F1	Ea=38.15	Ea= 45.19	Ea=53.89	Ea=54.47	Ea=62.85	Ea=64.79
	$A=1.63x10^{1}$	$A=4.4x10^{2}$	$A=3.47x10^{3}$	$A=3.36x10^{3}$	$A=2.0x10^{4}$	$A=2.89x10^{4}$
	$R^2=0.89747$	$R^2=0.9239$	$R^2=0.9598$	$R^2=0.9789$	$R^2=0.9633$	$R^2=0.9698$
F2	Ea=64.58	Ea=56.52	Ea= 69.33	Ea=68.96	Ea=81.12	Ea=84.36
	$A=1.19x10^{5}$	$A=6.98x10^{3}$	$A=1.39x10^{5}$	$A=1.06x10^{5}$	$A=1.45x10^{6}$	$A=2.65x10^{6}$
	$R^2=0.88294$	$R^2=0.8936$	$R^2=0.9291$	$R^2=0.9602$	$R^2=0.9307$	$R^2=0.9413$
R2	Ea=28.89	Ea=40.27	Ea=47.39	Ea=48.3	Ea=55.32	Ea=56.76
	$A=0.72x10^{1}$	$A=6.46x10^{1}$	$A=3.57x10^{2}$	$A=3.79x10^{2}$	$A=1.68x10^{3}$	$A=2.19x10^{3}$
	$R^2=0.90665$	$R^2=0.9368$	$R^2=0.9694$	$R^2=0.9828$	$R^2=0.9728$	$R^2=0.9771$
R3	Ea=31.69	Ea=41.86	Ea=49.47	Ea=50.27	Ea=57.71	Ea=59.3
	$A=1.01x10^{1}$	$A=6.4x10^{1}$	$A=3.95x10^{2}$	$A=4.08x10^{2}$	$A=1.97x10^{3}$	$A=2.67x10^{3}$
	$R^2=0.90512$	$R^2=0.9328$	$R^2=0.9668$	$R^2=0.9819$	$R^2=0.9703$	$R^2=0.9753$
$MPL^{1/3}$	Ea=31.69	Ea=41.86	Ea=49.47	Ea=50.27	Ea=57.71	Ea=59.3
	$A=3.03x10^{1}$	$A=1.93x10^{2}$	$A=1.18x10^{3}$	$A=1.22x10^{3}$	$A=5.92x10^{3}$	$A=7.99x10^{3}$
	$R^2=0.90512$	$R^2=0.9328$	$R^2=0.9668$	$R^2=0.9819$	$R^2=0.9703$	$R^2=0.9753$
$MPL^{1/2}$	Ea=28.89	Ea=40.27	Ea=47.39	Ea=48.3	Ea=55.32	Ea=56.76
	$A=1.45x10^{1}$	$A=1.29x10^{2}$	$A=7.14x10^{2}$	$A=7.57x10^{2}$	$A=3.35x10^{3}$	$A=4.39x10^{3}$
	$R^2=0.90665$	$R^2=0.9368$	$R^2=0.9694$	$R^2=0.9828$	$R^2=0.9728$	$R^2=0.9771$
$MPL^{2/3}$	Ea=26.39	Ea=39.74	Ea=45.42	Ea=46.4	Ea=53.04	Ea=54.34
	$A=0.74x10^{1}$	$A=9.03x10^{1}$	$A=4.39x10^{2}$	$A=4.77x10^{2}$	$A=1.95x10^{3}$	$A=2.48x10^{3}$
	$R^2=0.90658$	$R^2=0.9406$	$R^2=0.9715$	$R^2=0.9831$	$R^2=0.9748$	$R^2=0.9782$

(Table 5). Continued.

Code	Epoxy Resin	Epoxy + 4% Casuarina	Epoxy + 8% Casuarina	Epoxy+12% Casuarina	Epoxy+16% Casuarina	Epoxy+20% Casuarina
A2	Ea=38.15	Ea=45.19	Ea=53.89	Ea=54.47	Ea=62.85	Ea=64.79
	$A=8.14x10^{1}$	$A=2.19x10^{2}$	$A=1.73x10^{3}$	$A=1.68x10^{3}$	$A=1.0x10^{4}$	$A=1.44x10^{4}$
	$R^2=0.89747$	$R^2=0.9239$	$R^2=0.9598$	$R^2=0.9789$	$R^2=0.9633$	$R^2=0.9698$
A3	Ea=38.15	Ea=45.19	Ea=53.89	Ea=54.47	Ea=62.83	Ea=64.79
	$A=5.4x10^{1}$	$A=1.47x10^{2}$	$A=1.15x10^{3}$	$A=1.12x10^{3}$	$A=6.68x10^{3}$	$A=9.63x10^{3}$
	$R^2=0.89747$	$R^2=0.9239$	$R^2=0.9598$	$R^2=0.9789$	$R^2=0.9633$	$R^2=0.9698$
A4	Ea=38.15	Ea=45.19	Ea=53.89	Ea=54.47	Ea=62.85	Ea=64.79
	$A=4.07x10^{1}$	$A=1.09x10^{2}$	$A=8.66x10^{2}$	$A=8.41x10^{2}$	$A=5.0x10^{3}$	$A=7.22x10^{3}$
	$R^2=0.89747$	$R^2=0.9239$	$R^2=0.9598$	$R^2=0.9789$	$R^2=0.9633$	$R^2=0.9698$
Broido model	Ea=58.17	Ea=63.65	Ea=65.74	Ea=65.93	Ea=73.66	Ea=71.61
	$A=3.2x10^{5}$	$A=2.1x10^{4}$	$A=3.3x10^{4}$	$A=3.9x10^{4}$	$A=1.4x10^{6}$	$A=1.0x10^{5}$
	$R^2=0.9504$	$R^2=0.9782$	$R^2=0.9858$	$R^2=0.9762$	$R^2=0.9686$	$R^2=0.9596$
Horowitz model	Ea=67.56	Ea=69.5	Ea=73.46	Ea=75.16	Ea=83.85	Ea=85.01
	$A=1.06x10^{5}$	$A=4.9x10^{4}$	$A=5.3x10^{4}$	$A=6.1x10^{4}$	$A=5.6x10^{4}$	$A=6.1x10^{4}$
	$R^2=0.9566$	$R^2=0.9909$	$R^2=0.9919$	$R^2=0.9909$	$R^2=0.9889$	$R^2=0.9908$

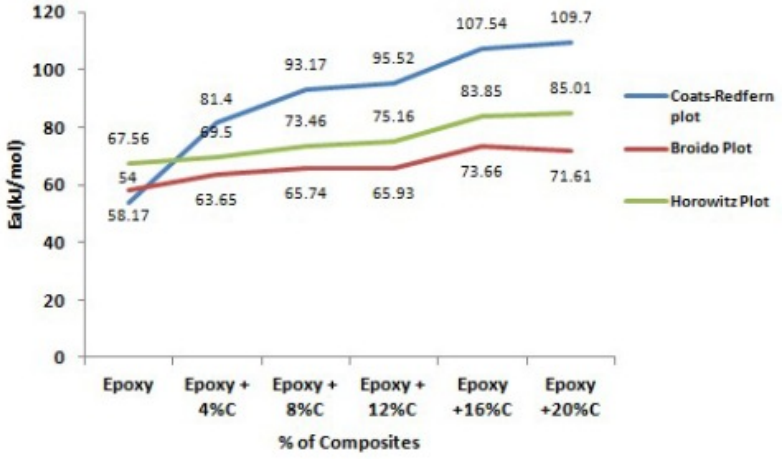

Figure 5: Comparison of activation energy between Coats, Broido and Horowitz Models.

Calculated activation energy was slightly high for Diffusion models (D1, D2&D3) when compared to reaction order models, contraction models and nucleation models. Studies reported by Mahmood *et al*. [30] revealed decomposition of bagasse fibre also followed One Dimensional Diffusion with high Ea due to less ash content and high volatile matter. Calculated activation energy and frequency factor for the composites showed an analogues trend with respect to all the models. Frequency factor is associated to the number of collisions occurring between molecules with requisite orientation takes place successfully. Table **5** portrays the frequency factor for One Dimensional Diffusion Model is in the range of $2x10^{5}$ to $7\ x10^{7}$. Figure **5** compares the activation energy values obtained using the Coats-Redfern model (One-Dimensional Diffusion Model), the Broido model and the Horowitz model, demonstrating that the calculated activation energies are consistent across all methods.

3.5. Thermodynamic Parameters for Thermal Decomposition of Epoxy Composites

Equations 3-5 were used to compute various thermodynamic parameters for all epoxy casuarina composites based on the frequency factor and activation energy acquired in the second phase of degradation. The results obtained for epoxy resin and epoxy casuarina fibre composites are listed in Table **6**. The findings showed that, in comparison to epoxy, casuarina epoxy composites had higher value of Ea, A, ΔH, ΔS and ΔG. It was also observed that as the percentage composition of fibre rises, the values of several thermodynamic parameters increase as well.

Table 6: Thermodynamic Parameters of Epoxy Casuarina Leaf Composites

Composites	Activation energy Ea(KJ/mol)	Frequency factor, A (s^{-1})	ΔH (KJ/mol)	ΔS (J/mol)	ΔG (KJ/mol)
Epoxy Resin	54	$1.23x10^3$	48.78	-191.95	169.4
Epoxy + 4% Casuarina fibre	81.40	$2.39x10^5$	76.17	-148.15	169.36
Epoxy + 8% Casuarina fibre	93.17	$3.5x10^6$	87.93	-125.85	167.20
Epoxy + 12% Casuarina fibre	95.52	$4.47x10^6$	90.28	-123.83	168.35
Epoxy + 16% Casuarinafibre	107.54	$4.89x10^7$	102.29	-103.94	167.88
Epoxy + 2% Casuarina fibre	109.7	$7.12x10^7$	104.45	-100.83	168.17

Negative ΔS values designated that the reaction is disorderly. The enthalpy of 76-104 KJ/mol and the Gibbs free energy of 167-169 KJ/mol were obtained via the best-fitting model (D1). The positive enthalpy change indicated that the reaction is endothermic, requiring energy as shown by the DSC graph and that the composites are stable compared to the resin. Each of the composite prepared showed a positive ΔG value, confirming that the reaction is not spontaneous, leading to an increase in the system's total energy. The magnitude of ΔG reflects how far the reaction is from equilibrium, with larger values indicating a greater shift required to reach equilibrium.

5. CONCLUSION

Epoxy casuarina composites with 4% to 20v/v % fibre compositions prepared by hand lay-up method were subjected into thermal study using TGA, DSC, DTA and DTG to study the suitability of casuarina epoxy composite at high temperature. The findings pronounced that the incorporation of 20 % casuarina fibre into the epoxy matrix, notably raises the peak temperature to 359°C in composite, comparison with the unreinforced epoxy resin's peak temperature of 355.4°C. DSC studies revealed that the glass transition temperature of the epoxy + 20 % casuarina fibre composite increased to 75.5°C, due to the increased space occupation which weakens molecular mobility, significantly higher than the 59°C of the epoxy resin. Coats- Redfern method, Broido method and Horowitz methods were employed to determine the activation energy. The calculated activation energy was in amicable with Coats- Redfern, Broido and Horowitz models. The study found that the energy of activation ranged from 81 to 109 KJ/mol and the frequency factor ranged from $2x10^5$ to $7\ x10^7$ for the best fitted One Dimensional Diffusion Model. The findings also showed that, in comparison to epoxy, epoxy casuarina composites had a higher value of Ea, A, ΔH, ΔS and ΔG and these parameters increases with increase in casuarina fibre composition. Thus, it is clear from this study, casuarina leaf can be used as a potential bio fibre to produce composites having high thermal stability and can be promoted widely in various engineering fields.

FUNDING SOURCES

Self funding this research did not receive any specific grant from funding agencies in the public, commercial, or not-for-profit sectors.

DECLARATION OF COMPETING INTEREST

The authors declare that they have no known competing financial interests or personal relationships that could have appeared to influence the work reported in this paper.

REFERENCES

[1] Arunprakash VR, Viswanathan R. Fabrication and characterization of Echinoidea spike particles and Kenaf natural fibrerein forced Azadirachta Indica blended epoxy multihybrid bio composite. Appl Sci Manuf 2019; 118: 317-326. https://doi.org/10.1016/j.compositesa.2019.01.008

[2] Zamani K, Kocaman S, Isik M, Soydal U, Ozmeral N, Ahmetli G. Water sorption, thermal and fire resistance properties of natural shell-based epoxy composites. J Appl Polym Sci 2022; 39(35). https://doi.org/10.1002/app.52835

[3] Yao F, Wu Q, Lei Y, Guo W, Xu Y. Thermal decomposition kinetics of natural fibers: Activation energy with dynamic thermogravimetric analysis. Polym Degrad Stab 2008; 93(1):90-98. https://doi.org/10.1016/j.polymdegradstab.2007.10.012

[4] Bera T, Acharya SK, Mishra P. Synthesis, mechanical and thermal properties of carbon black/epoxy composites. Int J Eng Sci Technol 2018; 10(4): 12-20. https://doi.org/10.4314/ijest.v10i4.2

[5] Ibrahim MS, Sapuanand SM, Faieza AA. Mechanical and thermal properties of composites from unsaturated polyester filled with oil palm ash. J Mech Eng Sci 2012; 2: 133-147. https://doi.org/10.15282/jmes.2.2012.1.0012

[6] Ben Samuel J, JulyesJaisingh S, Siva Kumar K, Mayakannan AV, Arunprakash VR. Visco-elastic, thermal, antimicrobial and dielectric behavior of areca fibre reinforced

nano silica and neem oil toughened epoxy resin bio composite. Silicon 2021; 13: 1703-1712. https://doi.org/10.1007/s12633-020-00569-0

[7] Parivendhan Inbakumar J, Ramesh S. Mechanical, wear and thermal behaviour of hemp fibre/egg shell particle reinforced epoxy resin bio composite. Trans Can Soc Mech Eng 2018; 42(3): 280-285. https://doi.org/10.1139/tcsme-2017-0079

[8] Alshammari BA, Al-Mubaddel FS, Karim MR, Hossain M, Al-Mutairi AS, Wilkinson AN. Polymers 2019; 11: 1411. https://doi.org/10.3390/polym11091411

[9] Khan R, Khare P, Baruah BP, Hazarika AK, Dey NC. Spectroscopic, Kinetic Studies of Polyaniline Flyash Composite. Adv Chem Engineer Sci2011; 1: 37-44. https://doi.org/10.4236/aces.2011.12007

[10] Al-Bayaty SA, Jubier NJ, Al-Uqaily RAH. Study ofthermal behavior and kinetics of epoxy/polystyrene composites by using TGA an DSC. J Xi'an Univ Archit Technol 2020; 12(3): 331.

[11] Farha AH, Al Naim AF, Mansour SA. Thermal Degradation of Polystyrene (PS) Nanocomposites Loaded with Sol Gel-Synthesized ZnO Nanorods. Polymers 2020; 12: 1935. https://doi.org/10.3390/polym12091935

[12] Abderrahim B, Abderrahman E, Mohamed A, Fatima T, Abdesselam T, Krim O. Kinetic Thermal Degradation of Cellulose, Polybutylene Succinate and a Green Composite Comparative Study. World J Environ Eng 2015; 3(4): 95-110.

[13] Chinnasamya V, Subramanib SP, Palaniappanc SK, Mylsamyd B, Aruchamye K. Characterization on thermal properties of glass fiber and kevlar fiber with modified epoxy hybrid composites. J Mater Res Technol 2020; 9(3): 3158-3167. https://doi.org/10.1016/j.jmrt.2020.01.061

[14] Rangappa SM, Siengchin S, Parameswaranpillai J, Jawai M, Ozbakkaloglu T. Lignocellulosic fiber reinforced composites Progress, performance, properties, applications, and future perspectives. Polym Compos 2022; 43(2): 645-691. https://doi.org/10.1002/pc.26413

[15] Du J, Gao L, Yang Y, Chen G, Guo S, Omran M, Chen J, Ruan R. Study on thermochemical characteristics properties and pyrolysis kinetics of the mixtures of waste corn stalk and pyrolusite. Bioresour Technol 2021; 324: 124660. https://doi.org/10.1016/j.biortech.2020.124660

[16] Sultania M, Srivatava D. The effect of CTBN concentrations on the kinetic parameters of decomposition of blends of epoxy resins modified with carboxyl terminated liquid copolymer. J Polym Environ 2011; 19: 950-956. https://doi.org/10.1007/s10924-011-0348-7

[17] Roudsari GM, Mohanty AK, Misra M. Study of the Curing Kinetics of Epoxy Resins with Biobased Hardener and Epoxidized Soybean Oil. ACS Sustainable Chem Eng 2014; 2: 2111−2116. https://doi.org/10.1021/sc500176z

[18] Borsoi C, Zimmernnam MVG, Zattera AJ. Thermal degradation behavior of cellulose nanofibers and nanowhiskers. J Therm Anal Calorim 2016; 126: 1867-78. https://doi.org/10.1007/s10973-016-5653-x

[19] Kumar S, Gulati K, Singh SKA. Study of thermal degradation of Varieties of Plywood by Using Thermogravimetry under Nitrogen Atmosphere. Int JADV Sci Resmana 2018; 3 (8).

[20] Vishnu R, Revathi R. Studies on physical, chemical and fibre morphological parameters of three pulpwood species viz. Eucalyptus, Melia and Casuarina for pulp and paper making. Int J Chem Stud 2019; 7(5): 3155-3162

[21] Coats AW, Redfern JP. Kinetic Parameters from Thermogravimetric Data. Nature 1964; 201: 68-69. https://doi.org/10.1038/201068a0

[22] Broido A. A simple, sensitive graphical method of treating thermogravimetric analysis data. J Polym Sci Part A 1969; 7(10):1761-73. https://doi.org/10.1002/pol.1969.160071012

[23] Horowitz HH, Metzger G. A New Analysis of Thermogravimetric Traces. Anal Chem 1963; 35(10): 1464-1468. https://doi.org/10.1021/ac60203a013

[24] Ebrahimi-Kahrizsangi R, Abbasi MH. TranNonferrous met Soc China 2008; 18(1): 217-221. https://doi.org/10.1016/S1003-6326(08)60039-4

[25] Alwani MS, Abdul Khalil HPS, Sulaiman O, Islam MN Dungani R. An approach to using agricultural waste fibres in biocomposites application: Thermogravimetric analysis and activation energy study. Bio Res 2014; 9(1): 218-230. https://doi.org/10.15376/biores.9.1.218-230

[26] Glowinska E, Datta J, Parcheta P. Effect of sisal fiber filler on thermal properties of bio-based polyurethane composites. J Therm Anal Calorim 2017; 130:113-122. https://doi.org/10.1007/s10973-017-6293-5

[27] Acikalin K. Thermogravimetric analysis of walnut shell as pyrolysis feedstock. J Therm Anal Calorim 2011; 105(1): 145-150. https://doi.org/10.1007/s10973-010-1267-x

[28] Zhang X, Huang R. Thermal Decomposition Kinetics of Basalt Fiber Reinforced Wood Polymer Composites. Polymers 2020; 12: 2283. https://doi.org/10.3390/polym12102283

[29] Titok V, Leontiev V, Shostak L, Khotyleva. Thermogravimetric Analysis of the Flax Bast Fibre Bundle. J Nat Fibers 2006; 3(1): 35-41. https://doi.org/10.1300/J395v03n01_04

[30] Mahmood H, Shakeel A, Abdullah A, Khan MI, Moniruzzaman M. A Comparative Study on Suitability of Model-Free and Model-Fitting Kinetic Methods to Non-Isothermal Degradation of Lignocellulosic Materials. Polymers 2021; 13: 2504. https://doi.org/10.3390/polym13152504

Received on 02-07-2024 Accepted on 25-07-2024 Published on 02-09-2024

https://doi.org/10.6000/1929-5995.2024.13.09